Pediatr Radiol (2011) 41:1536–1544
DOI 10.1007/s00247-011-2196-y

ORIGINAL ARTICLE

Combined respiratory and cardiac triggering improves blood pool contrast-enhanced pediatric cardiovascular MRI

Shreyas S. Vasanawala · Frandics P. Chan · Beverley Newman · Marcus T. Alley

Received: 22 March 2011 / Revised: 27 May 2011 / Accepted: 2 June 2011 / Published online: 24 July 2011

Abstract
Background Contrast-enhanced cardiac MRA suffers from cardiac motion artifacts and often requires a breath-hold.
Objective This work develops and evaluates a blood pool contrast-enhanced combined respiratory- and ECG-triggered MRA method.
Materials and methods An SPGR sequence was modified to enable combined cardiac and respiratory triggering on a 1.5-T scanner. Twenty-three consecutive children referred for pediatric heart disease receiving gadofosveset were recruited in HIPAA-compliant fashion with IRB approval and informed consent. Children underwent standard non-triggered contrast-enhanced MRA with or without suspended respiration. Additionally, a free-breathing-triggered MRA was acquired. Triggered and non-triggered studies were presented in blinded random order independently to two radiologists twice. Anatomical structure delineation was graded for each triggered and non-triggered acquisition and the visual quality on triggered MRA was compared directly to that on non-triggered MRA.
Results Triggered images received higher scores from each radiologist for all anatomical structures on each of the two reading sessions (Wilcoxon rank sum test, $P<0.05$). In direct comparison, triggered images were preferred over non-triggered images for delineating cardiac structures, with most comparisons reaching statistical significance (binomial test, $P<0.05$).
Conclusion Combined cardiac and respiratory triggering, enabled by a blood pool contrast agent, improves delineation of most anatomical structures in pediatric cardiovascular MRA.

Keywords Gadofosveset/Ablavar · Cardiac MRI · MRA · Gating · Children

Introduction

Pediatric cardiovascular MRI is challenged by motion artifacts resulting from cardiac pulsation and respiration. Respiratory motion can be eliminated by suspended respiration, either through voluntary breath-holding by a cooperative patient or through apnea under general anesthesia. When obtained through general anesthesia, a period of suspended respiration requires a deeper degree of anesthesia than otherwise needed for MRI, and as a result an artificial airway is often required [1]. Though the associated risks of anesthesia are low [2], it is prudent to minimize use of deep sedation.

Cardiac motion is managed through EKG synchronization for bright- and black-blood imaging, as well as phase-

S. S. Vasanawala (✉) · B. Newman
Department of Radiology, Stanford University School of Medicine,
Lucile Packard Children's Hospital,
725 Welch Road, Room 1679,
Stanford, CA 94305-5913, USA
e-mail: vasanawala@stanford.edu

F. P. Chan
Department of Radiology,
Stanford University School of Medicine,
Stanford, CA, USA

M. T. Alley
Department of Radiology,
Stanford University School of Medicine, Lucas MRS Center,
Stanford, CA, USA

contrast sequences [3]. With most of the available MR sequences and contrast agents, EKG triggering is impractical for first-pass, contrast-enhanced MR angiography (MRA) because of the marked lengthening of data acquisition beyond the duration of the contrast bolus.

Blood pool MRI contrast agents have been under development for some time, including an agent originally referred to as MS-325 [4, 5] but with the generic name of gadofosveset. Gadofosveset was originally used in humans in the late 1990s [6] and has been available in Europe under the tradename of Vasovist. More recently gadofosveset trisodium has obtained U.S. Food and Drug Administration approval for aortoiliac MRA in adults. The agent reversibly binds to albumin, yielding a higher relaxivity as well as prolonged blood pool residence [7]. Initial work exploring the use of this agent for cardiac imaging was focused on the adult population [8–11], with promising results. More recently, evaluation in children has focused on enhancing bright-blood balanced steady-state imaging, also with promising results [12].

This work develops a combined respiratory- and ECG-triggered spoiled gradient recalled echo (SPGR) MRA method and assesses the resulting delineation of cardiovascular anatomy compared with traditional non-triggered SPGR MRA in children undergoing cardiac MRI with a blood pool contrast agent.

Materials and methods

A spoiled gradient recalled echo sequence (SPGR) was modified to enable cardiac triggering, respiratory triggering and fractional acceleration with Poisson-disc sampling [13]. Pulse sequence parameters include a flip angle of 20°, bandwidth 62.5 kHz, frequency and phase matrix each ranging from 300 to 384, field of view 20–35 cm, slice thickness 1–2.2 mm. All imaging was performed at 1.5T (GE Signa HDxt; GE Healthcare, Milwaukee, WI, USA) with an eight-channel cardiac phased-array receiver coil.

Twenty-three consecutive children referred for evaluation of pediatric heart disease who received single-dose gadofosveset (Ablavar; Lantheus Medical Imaging, Billerica, MA, USA) were prospectively recruited with IRB approval and informed consent. The study was HIPAA-compliant. The use of gadofosveset in children represents an off-label application and is associated with QT prolongation as well as risk of arrhythmias. Single-dose gadofosveset (0.12 mL/kg of 0.25 mmol formulation, i.e. 0.03 mmol/kg) was administered intravenously. Doses of less than 10 mL were first diluted in sterile saline to a total volume of 10 mL. Contrast agent was power-injected at rate of 1 mL/s, followed by a saline flush of 20 mL.

Children underwent standard non-triggered contrast-enhanced MRA with or without suspended respiration, depending on each patient's clinical condition and imaging requirements. Additionally, a free-breathing MRA was acquired with cardiac and respiratory triggering. Respiratory signal was generated by monitoring air pressure from a mechanical bellow placed across the chest of the patient or from the ventilation system connected to the patient. The respiratory trigger delay and acquisition window were each set at 30% of the respiratory cycle. For six children, the triggered MRA preceded the non-triggered MRA, and the latter was imaged during equilibrium contrast phase. For the remaining 17 children, the non-triggered MRA was obtained first. The first non-triggered acquisition was at arterial phase, with scan delay chosen to ensure that the center of k-space was obtained 18 s after half the bolus was administered. Since the acquisition had sequential encoding, scan delay in seconds for a 10 mL bolus of contrast was $18+(10/2)-(\text{scantime})/2$. Eighteen seconds has been used in this calculation because we have noted that it represents the peak enhancement from timing boluses for the vast majority of patients. Upon completion of the arterial phase, the non-triggered acquisition was repeated at equilibrium phase.

For two children, the acquisition scan plane was changed from sagittal for non-triggered MRA to coronal for triggered MRA to optimize image quality for diagnostic reasons. For all remaining children, the coronal plane was used and the scan parameters were fixed except for acceleration factors. The fraction of the RR interval used for data acquisition varied from 30% to 50% depending on the heart rate, with the higher percentage used at a lower heart rate. Trigger delay was at 20% of RR cycle after the R wave. Acceleration factors were increased for triggered imaging in two cases to keep scan time less than 6 min.

For children unable to cooperate during MRI, general anesthesia with deep sedation was performed by anesthesiologists specialized in cardiac patient care. Airways were maintained by endotracheal intubation or laryngeal airway mask. Deep sedation was maintained by a combination of propofol intravenous infusion and anesthetic gas. Respiration was mechanically ventilated during the study.

Triggered and non-triggered MRA studies were presented in anonymized fashion and randomized order independently to two radiologists who each had dedicated experience in cardiovascular imaging for 10 years. For exams with both arterial phase and equilibrium non-triggered images, equilibrium phase images were evaluated. Studies were presented on a 3D-postprocessing viewer

(Osirix) where the readers could examine data interactively in coronal, axial or sagittal planes. After 2 weeks of separation, the studies were randomized again and reviewed in a second session. In each session, visual quality of clinically important vascular structures such as the aorta, pulmonary trunk, pulmonary veins, and inferior and superior venae cavae were graded on a five-point scale (Table 1) for each triggered and non-triggered acquisition. Then for each vascular structure from each child, the visual quality of the triggered MRA was compared directly to that of the non-triggered MRA, also on a five-point scale: left series with more delineation, left series preferred, left and right series equivalent, right series preferred, and right series with more delineation. Finally, the severity of phase ghosting from cardiac motion was compared between the paired triggered and non-triggered MRAs on the same five-point scale.

To test the null hypothesis that there is no significant difference between triggered and non-triggered gradings for each anatomical structure, a Wilcoxon matched-pairs rank sum test was employed. To test the null hypothesis that triggered images are not improved over non-triggered images when directly compared, a binomial test was performed. A significance level of 0.05 was used. Finally, inter-observer and intra-observer agreement and correlations were determined.

Results

Patient ages ranged from 4 months to 16 years with a mean of 4.5 years. Twelve girls and 11 boys were recruited. Mean scan time for triggered scans was 4.4 min (range 2.9–6.2 min), compared with approximately 30 s for non-triggered acquisitions. In six cases, the non-triggered images had poor contrast enhancement of the hepatic veins because of early contrast phase, and for the ensuing analysis involving the hepatic veins these cases were excluded.

The fraction of cases with various scores of image quality for each anatomical structure is shown for triggered and non-triggered MRA studies (Fig. 1). Triggered images were given higher scores by each radiologist for all anatomical structures and cardiac ghosting on each of the two reading sessions (Wilcoxon rank sum test, $P<0.05$ in all cases). The mean scores for triggered and non-triggered

Table 1 Grading scale with criteria for evaluating anatomical structures

Grading	Hepatic vein confluence	Pulmonary veins	Coronary arteries
Outstanding	No perceptible motion artifact	Can assess peripheral stenosis	Can see beyond proximal 1/3
Excellent	Margins of HVs and IVC clearly seen	Can assess ostial stenosis of all veins	Can see proximal course beyond great arteries
Diagnostic	Can assess obstruction	Can assess ostial stenosis of at least 50% of veins	Can see origin of each coronary
Limited	Can count veins	Can count veins	Can see left or right coronary
Nondiagnostic	Cannot count veins	Cannot count veins	Cannot see either artery
Grading	**RV trabeculation**	**Ventricular septum**	**Ascending aorta**
Outstanding	No motion artifact, clear trabecular delineation	Can exclude perimembranous VSD	No artifact
Excellent	Anterior papillary muscle seen	Can assess muscular VSD	Clear definition of margins
Diagnostic	Can distinguish right from left ventricle	Can assess AV canal defect	Can measure aorta at level of branch PAs
Limited	Cannot determine right/left ventricle	Septum seen	Cannot assess stenosis or aneurysm
Nondiagnostic	Cannot see ventricle	Cannot see ventricle	Cannot see ascending aorta
Grading	**Pulmonary arteries**	**Aortic valve**	**Aortic arch**
Outstanding	Can assess stenosis in >50% segmental vessels	Can see aortic valve leaflets	Can assess for stenosis
Excellent	Can assess stenosis >50% lobar vessels	Can measure aortic annulus and assess vegetations	Can see all cervical vessels
Diagnostic	Can assess RPA/LPA stenosis	Can measure aortic valve annulus	Can assess for PDA
Limited	Cannot assess pulmonary trunk stenosis	Cannot measure size at the sinus of Valsalva	Can tell left versus right
Nondiagnostic	Cannot see pulmonary trunk	Cannot see aortic valve	Cannot see arch

MRA studies show very similar results for non-triggered breath-hold studies and non-triggered free-breathing studies (Fig. 1).

Figure 2 illustrates the direct comparison between triggered and non-triggered images, showing a strong preference for the triggered images. Triggered images were more likely to be preferred (Table 2) than non-triggered images for most structures by both readers (one-sided binomial test, $P<0.05$). For one radiologist, the ventricular septum, coronary arteries and aortic arch trended toward preference of triggered images but did not reach a statistical level of significance ($P=0.105$) for one reading session; for the second reading session the coronary arteries again trended preference ($P=0.105$). For the other radiologist, the ascending aorta and arch failed to reach significance ($P=0.33$ and 0.89, respectively) on one session, with the aortic arch again showing no clear benefit of triggering in the second session ($P=0.33$).

Intra- and inter-observer agreement for scores of quality of delineation were 82–97% for all anatomical structures

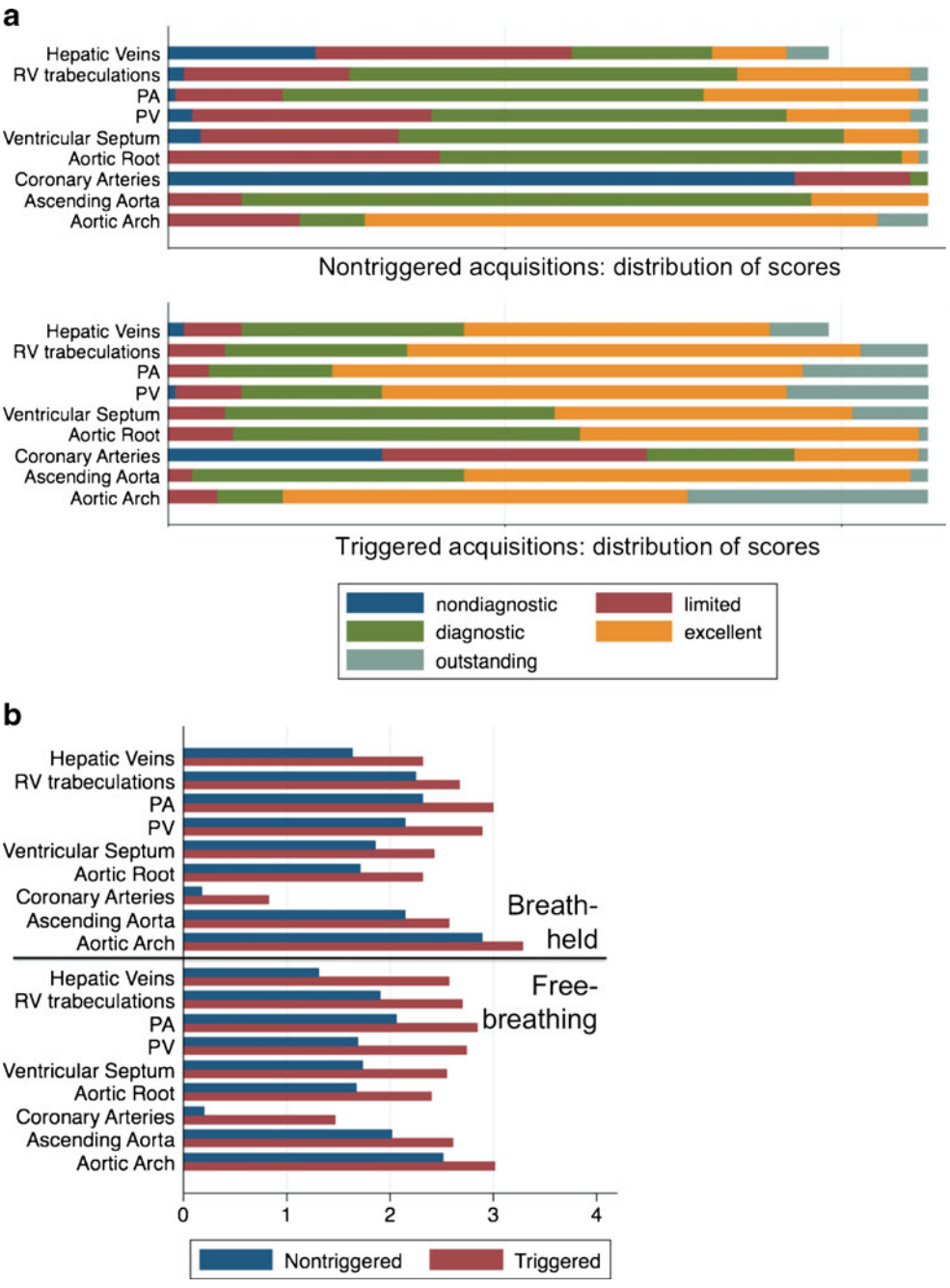

Fig. 1 Triggered vs. non-triggered MRA grading. **a** Combined frequency of scores from both observers for each category of the grading scale. Top chart shows non-triggered MRA scores; bottom shows triggered MRA scores. Note the increased number of excellent and outstanding scores for each anatomical structure on the triggered MRA. **b** Mean scores of image quality for non-triggered and triggered images, with score of 0 equivalent to a nondiagnostic rating and a score of 4 reflecting an outstanding rating

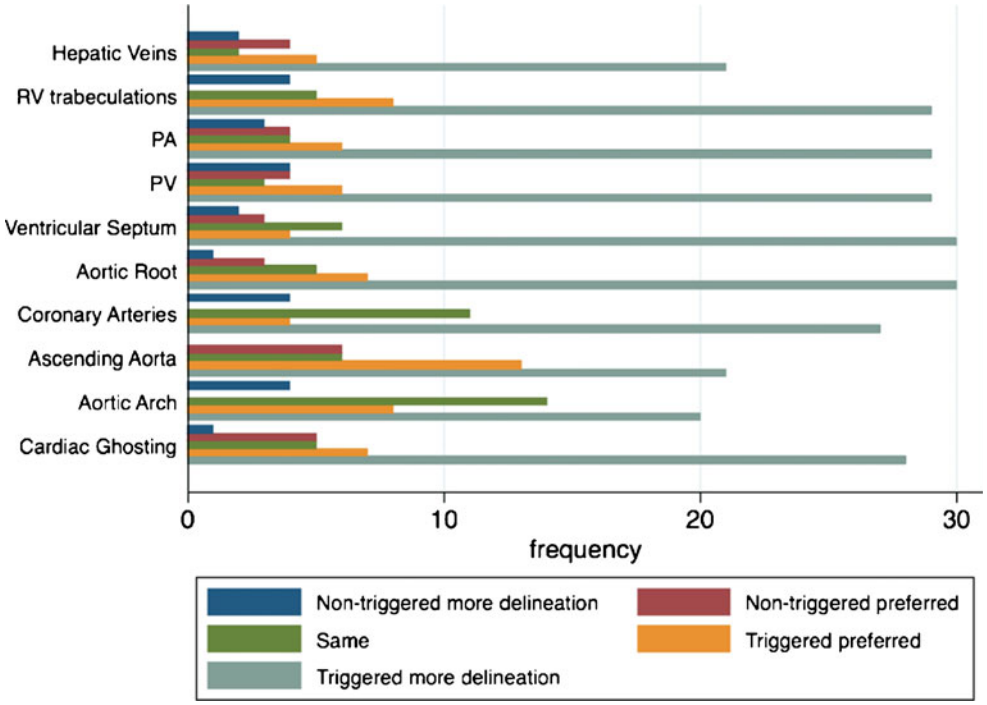

Fig. 2 Comparison of triggered MRA with non-triggered MRA. Combined frequency for both observers for each category of comparison is shown

and acquisition types, except for one outlier: coronary artery inter-observer agreement on triggered images was 71%. Intra- and interobserver correlations were mostly moderate to strong, with the exception of poor correlations for the coronary arteries, as seen in Table 3.

A representative example is shown in Fig. 3, which highlights improved delineation of the ventricular septum. Further, Fig. 4 shows the same patient but at a more superior slice level showing delineation of the coronary arteries in the atrio-ventricular grooves. Figure 5 shows a representative image from another child highlighting improved delineation of the aortic root, main pulmonary artery and a central catheter. Further, Fig. 6 highlights similar delineation of extra-cardiac structures. Finally, Fig. 7 shows an example of the technique compared with a suspended respiration acquisition.

Table 2 Percentage of comparison scores favoring triggered images over non-triggered images

Anatomical structure	Percentage favorable on triggered MRA
Right ventricle	84
Aortic valve	80
Ventricular septum	80
Pulmonary arteries	79
Hepatic veins	79
Pulmonary veins	78
Ascending aorta	71
Coronary arteries	68
Aortic arch	59

Discussion

This work compares two methods of MRA: non-triggered and triggered. Non-triggered MRA benefits from suspended respiration, permits first-pass selective angiography, suffers from significant cardiac ghosting artifacts, and can be performed with most MR contrast agents. Triggered MRA benefits from a stable breathing pattern, avoids a contrast test bolus for precise acquisition timing, provides equilibrium-phase MRA only, allows lighter general anesthesia requirements, takes longer to acquire, and thus requires a blood pool contrast agent. This work shows significantly improved delineation of most anatomical structures in pediatric cardiovascular MRA when cardiac and respiratory motions are minimized through combined triggering.

Intracardiac structures are known to be relatively poorly delineated on contrast-enhanced MRA. In this study, we show there is marked improvement in the definition of intracardiac structures when using combined cardiac- and respiratory-triggered MRA. However, although the coronary arteries were better seen on triggered versus non-triggered scans, there were still only a few cases in which

Table 3 Intra-observer and inter-observer correlation coefficients

Anatomical structure	Breath-held non-triggered			Free-breathing non-triggered			Free-breathing triggered		
	Intra-observer correlation		Inter-observer	Intra-observer correlation		Inter-observer	Intra-observer correlation		Inter-observer
	Reader 1	Reader 2		Reader 1	Reader 2		Reader 1	Reader 2	
Hepatic veins	0.94	0.93	0.97	0.76	0.65	0.80	0.72	0.79	0.77
RV trabeculations	0.71	0.89	0.63	0.46	0.73	0.73	0.30	0.55	0.59
PA	0.38	0.74	0.75	0.52	0.66	0.45	0.45	0.46	0.32
PV	0.78	0.80	0.77	0.38	0.54	0.00	0.43	0.73	0.45
Venticular septum	0.29	0.92	0.90	0.52	0.64	0.23	0.27	0.63	0.41
Aortic valve	1.00	0.43	0.29	0.73	0.92	0.57	0.72	0.73	0.64
Coronary arteries	0.63	0.00	0.00	0.00	0.75	0.62	0.64	0.71	0.37
Ascending aorta	0.63	0.90	0.37	0.02	0.76	0.31	0.55	0.65	0.10
Aortic arch	0.69	0.76	0.56	0.78	0.84	0.78	0.78	0.74	0.57

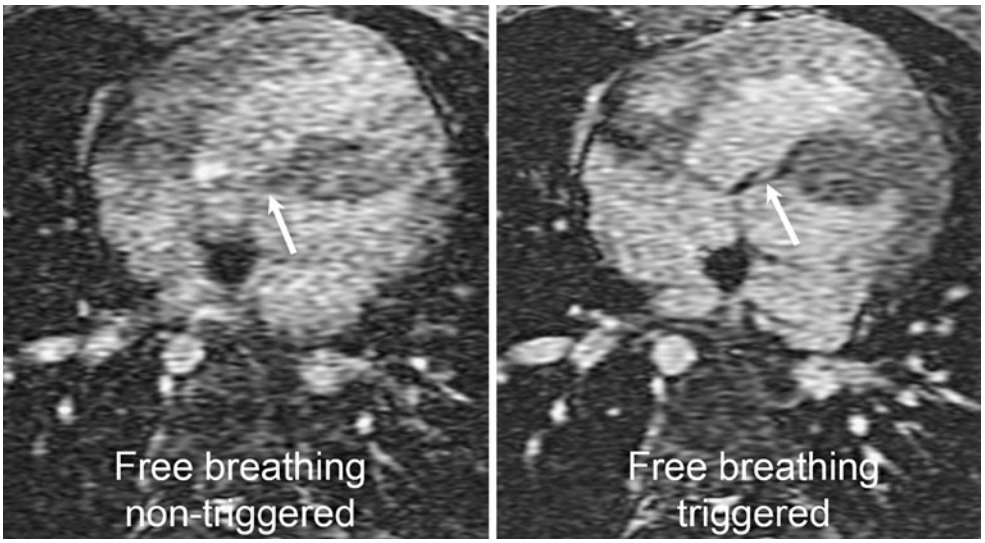

Fig. 3 Axial reformats of a 7-year-old with transposition of the great arteries (D-TGA) after atrial switch and pulmonary artery banding. Compare demonstration of intra-cardiac anatomy, particularly the intact membranous septum (*arrows*)

Fig. 4 Same child as Fig. 3. With triggering, coronary arteries can be seen (*arrows*)

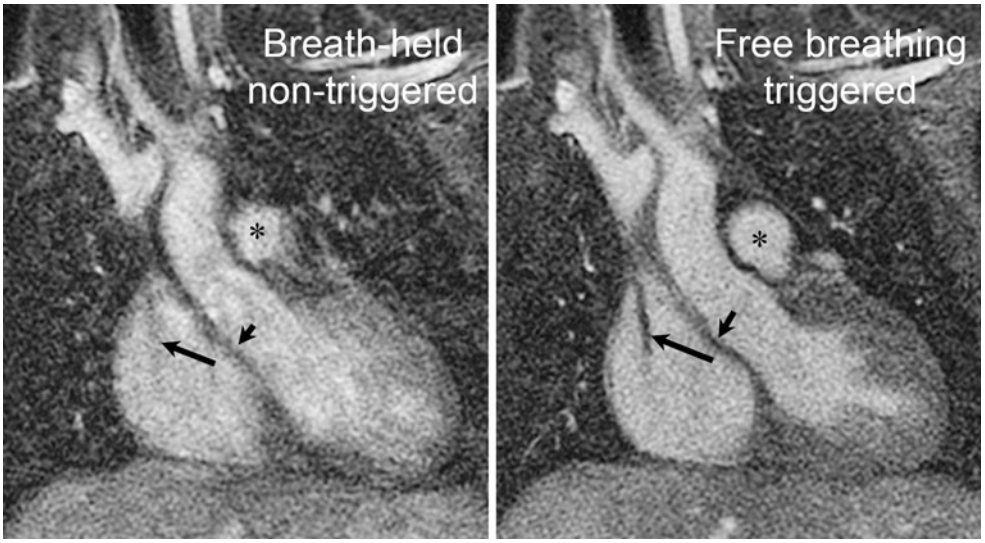

Fig. 5 A 7-year-old girl with pulmonary hypertension. Note improved delineation of a central venous catheter (*long arrow*), aortic root (*short arrow*) and pulmonary artery (*black* *) with triggering

the coronary visualization was considered excellent or outstanding. The greater anatomical detail afforded by a triggered MR angiographic study is likely to be especially important in small children with complex heart disease where high-quality MRA images with 2D and 3D reconstructions might obviate the need for other imaging studies with ionizing radiation exposure such as cardiac catheterization and gated CTA. Although triggered scans took longer to acquire, the additional time expended was small relative to the typical overall exam time of a cardiac MRI.

A potential alternative approach to MRA is unenhanced navigated cardiac-triggered balanced steady-state imaging (bSSFP), which has routinely been used for coronary artery imaging. Similar to the method presented in this work, bSSFP delineates intra-cardiac anatomy well. However, it suffers inhomogeneity-related artifacts, so delineating peripheral pulmonary vessels is challenging. Further, our clinical population often has a history of cardiac surgery or catheter interventions, which results in severe metallic artifacts on bSSFP images.

Similar to bSSFP, with the triggered MRA technique described here first-pass selective angiograms are not obtained. Thus, deciphering arteries from veins can be more challenging and require detailed knowledge of cardiothoracic anatomy and complex congenital heart disease. Further, this might limit the degree to which some structures can be volume-rendered.

With current clinically approved gradients, acquisition of thoracic contrast-enhanced MRA with cardiac gating at a resolution high enough to depict small structures such as coronary artery origins requires a lengthy scan time beyond a practical breath-hold. Thus, respiratory compensation

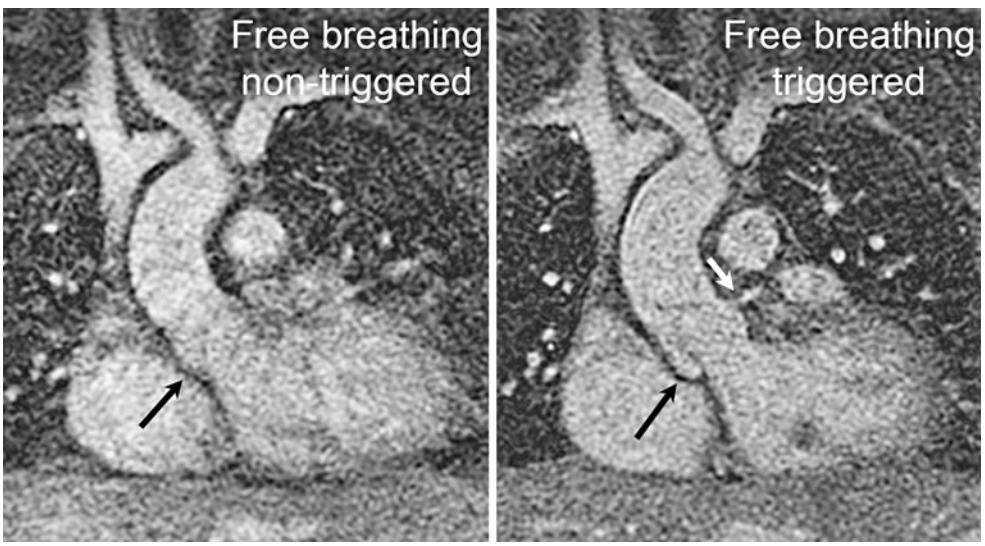

Fig. 6 A 3-year-old with repaired tetralogy. Note the depiction of the left coronary artery (white arrow) and aortic root (*black arrow*)

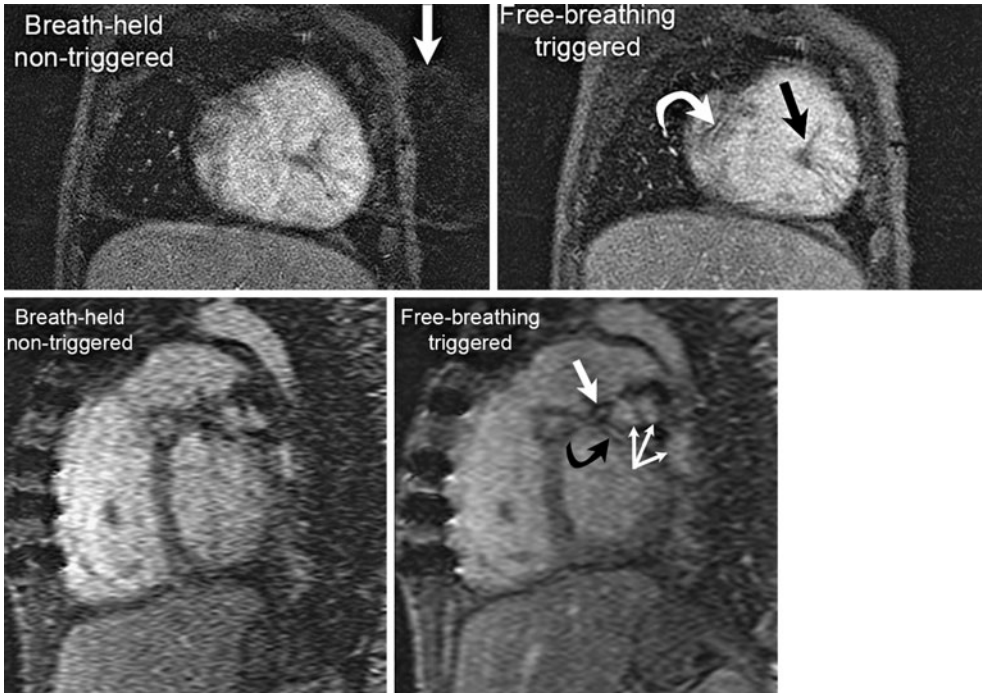

Fig 7 Another 3-year-old boy with repaired tetralogy. Top: Source coronal images. Note diminished cardiac ghosting artifacts (*white arrow*), improved delineation of right coronary artery (*curved arrow*), and right ventricular trabeculations (*solid black arrow*). Bottom: Sagittal reformats with triggered images show left anterior descending coronary (*white arrow*), left circumflex coronary artery (*curved black arrow*) and left pulmonary veins (*solid white arrows*)

with either navigation or triggering is required, further lengthening scan time. Thus, to gain the benefit of non-breath-hold MRA study, an intravascular contrast agent such as gadofosveset is needed to maintain a constant blood pool signal. However, by combining respiratory and cardiac triggering with a blood pool contrast agent, the typical constraints of MRA are removed. Bolus duration and breath-hold capacity no longer limit resolution and anatomical coverage. Rather, scan time and SNR become larger concerns. Though our triggered scans were limited to 6-min acquisitions, longer acquisitions could be employed to improve spatial resolution, further diminish motion artifacts, or improve SNR. These longer acquisitions might replace other sequences of the cardiac MR exam that are targeted to anatomical delineation, thereby compensating for the increased scan time.

Though intracardiac anatomy might be delineated to greater extent with triggered MRA, various clinical applications might benefit from selective first-pass angiography. These include coarctation, where 3D volume rendering might be improved by high SNR. Other applications, such as aortic root aneurysm in the context of Marfans syndrome might benefit from triggering, as might other cases requiring surgical planning of outlet reconstruction. Additionally, cases in which timing acquisition of imaging after contrast agent administration, such as Fontan circuits, might benefit from a blood pool contrast agent. Decision-making for the use of blood pool angiography might then best involve consideration of the clinical imaging need to assess moving structures, the ease of avoiding suspended respiration and the increased cost of blood pool agent. At the moment, diagnosis of aberrant coronary artery is probably not reliable with either approach, though better optimization of trigger windows would improve this application.

The study has several limitations. First, scan parameters are not uniform in all patients although their adjustments reflect “best clinical practice.” They were optimized for clinical indication, patient size and heart rate. The resulting variation in scan parameters diminishes clean comparison of two techniques but on the other hand results in a study assessing how the two techniques would be used in a practical clinical setting. Second, image analysis was performed in orthogonal planes at fixed slice thickness only. Effects on additional imaging post-processing methods, such as oblique reformation, maximal-intensity projection, and volume rendering, were not evaluated in this study. Third, in the triggered study, the cardiac window of data acquisition has not been optimized for specific anatomical structures. For example, with further adjustment of the cardiac triggering parameters, it might be possible to visualize the coronary arteries reliably. Finally, a somewhat arbitrary scan time limitation of 6 min for triggered MRA was imposed for this study, which might not be an optimal choice for various clinical

situations. However, the promising results of this initial study motivate further evaluation of triggered MRA using a blood pool contrast agent.

Conclusion

Combined cardiac/respiratory triggering, enabled by a blood pool contrast agent, improves delineation of anatomical structures in pediatric cardiovascular MRA.

Acknowledgements Authors gratefully acknowledge support from NIH grant RR09794-15, NIH grant R01 EB009690, and the Tashia and John Morgridge Foundation. Authors also thank Jennifer Vancil for skillful manuscript preparation assistance.

References

1. Sarikouch S, Schaeffler R, Korperich H et al (2009) Cardiovascular magnetic resonance imaging for intensive care infants: safe and effective? Pediatr Cardiol 30:146–152
2. Dorfman AL, Odegard KC, Powell AJ et al (2007) Risk factors for adverse events during cardiovascular magnetic resonance in congenital heart disease. J Cardiovasc Magn Reson 9:793–798
3. Lanzer P, Botvinick EH, Schiller NB et al (1984) Cardiac imaging using gated magnetic resonance. Radiology 150:121–127
4. Lauffer RB, Parmelee DJ, Ouellet HS et al (1996) MS-325: a small-molecule vascular imaging agent for magnetic resonance imaging. Acad Radiol 3(Suppl 2):S356–358
5. Lin W, Abendschein DR, Haacke EM (1997) Contrast-enhanced magnetic resonance angiography of carotid arterial wall in pigs. J Magn Reson Imaging 7:183–190
6. Grist TM, Korosec FR, Peters DC et al (1998) Steady-state and dynamic MR angiography with MS-325: initial experience in humans. Radiology 207:539–544
7. (2004) Gadofosveset: MS 325, MS 32520, Vasovist, ZK 236018. Drugs R D 5:339–342
8. Prompona M, Cyran C, Nikolaou K et al (2010) Contrast-enhanced whole-heart coronary MRA using gadofosveset 3.0 T versus 1.5 T. Acad Radiol 17:862–870
9. Prompona M, Cyran C, Nikolaou K et al (2009) Contrast-enhanced whole-heart MR coronary angiography at 3.0 T using the intravascular contrast agent gadofosveset. Invest Radiol 44:369–374
10. Stuber M, Botnar RM, Danias PG et al (1999) Contrast agent-enhanced, free-breathing, three-dimensional coronary magnetic resonance angiography. J Magn Reson Imaging 10:790–799
11. Wagner M, Rief M, Asbach P et al (2010) Gadofosveset trisodium-enhanced magnetic resonance angiography of the left atrium—a feasibility study. Eur J Radiol 75:166–172
12. Naehle CP, Kaestner M, Muller A et al (2010) First-pass and steady-state MR angiography of thoracic vasculature in children and adolescents. JACC Cardiovasc Imaging 3:504–513
13. Vasanawala SS, Alley MT, Hargreaves BA et al (2010) Improved pediatric MR imaging with compressed sensing. Radiology 256:607–616